Deformation structures in the Muschelkalk Anhydrites of the Schafisheim Well (Jura overthrust, northern Switzerland)

Autor(en): **Jordan, Peter / Nüesch, Rolf**

Objekttyp: **Article**

Zeitschrift: **Eclogae Geologicae Helvetiae**

Band (Jahr): **82 (1989)**

Heft 2

PDF erstellt am: **21.07.2024**

Persistenter Link: https://doi.org/10.5169/seals-166384

Eclogae geol. Helv. 82/2: 429–454 (1989)

0012-9402/89/020429-26 $ 1.50 + 0.20/0

Deformation Structures in the Muschelkalk Anhydrites of the Schafisheim Well (Jura Overthrust, Northern Switzerland)

By Peter Jordan[1]) and Rolf Nüesch[2])

ABSTRACT

Meso- and microstructures within the evaporite Main Décollement, which was completely recovered at the Schafisheim Nagra-well, show that strain was not uniformly accommodated by the various layers and lithologies. Within some sequences sedimentary structures are preserved while, often within a few decimeters, other sequences are highly strained. In some distinct horizons of the "layered sulpharenite", mylonite-like fabrics developed at low temperatures (ca. 80 °C), high strain rates (1.8 to $13 \cdot 10^{-13}$ s^{-1}), and within three meters of a thick salt layer. Microstructures suggest that flow stress of anhydrite is not only controlled by temperature, strain rate, and grain size, but also by the impurity content (commonly micro-crystalline dolomite, magnesite, or quartz). Adjacent to pure ductile anhydrites, anhydrites with ≥ 20% impurities show a high competence contrast, while anhydrites with ≥ 25% impurities even behaved brittle. Although still documenting a high strain, the grain fabric was post-kinematically annealed to such an extent that deformation mechanisms could not be determined any more.

ZUSAMMENFASSUNG

Die Muschelkalk-Evaporite, Hauptabscherhorizont der Jura-Überschiebung, wurden in der Nagra-Tiefbohrung Schafisheim (AG) vollständig gekernt. Meso- bis mikroskopische Untersuchungen zeigen, dass die verschiedenen Anhydrit-Lagen, bedingt durch abweichende Fliessfestigkeit, in unterschiedlichem Masse deformiert wurde. Die Fliessfestigkeit wird dabei nicht nur durch die Korngrösse, sondern auch durch den Grad der Verunreinigung kontrolliert. Als Verunreinigungen treten in Schafisheim neben geringen Anteilen von Quarz, Tonmineralien, Kalzit und Halit überwiegend feinkristalline Dolomite oder Magnesite auf. Die beiden Karbonate treten aber nie gemeinsam auf. In direkter Nachbarschaft zu reinen, hochduktilen Anhydriten verhalten sich schon relativ geringfügig verunreinigte (≥ 25%) Anhydrite spröde.

Die Anhydrite zeigen örtlich sehr starke Deformation. In den «Geschichteten Sulphareniten» haben sich Mylonit-ähnliche Gefüge ausgebildet. Dies ist in doppeltem Masse bemerkenswert, da diese Mylonitisierung nicht nur bei relativ tiefen Temperaturen (ca. 80 °C) und hohen Scherraten (1.8 bis $13 \cdot 10^{-13}$ s^{-1}), sondern auch noch in direkter Nachbarschaft zu einem mächtigen Salzlager stattgefunden haben muss. Das Kristallgefüge des Anhydrites zeigt zwar meist noch starke Deformation an, ist in der Regel aber durch postkinematische, statische Rekristallisation so verändert, dass sich die ursprünglich wirksamen Deformationsmechanismen nicht mehr feststellen lassen.

Introduction

The Jura mountains are the result of a northwest movement of the Mesozoic-Cenozoic sedimentary prism in the Alpine foreland during the late Tertiary ("Fernschub": Laubscher 1961, see also Fig. 1). Since most of the overthrusts and folds are rooted in

[1]) Geologisches Institut der Universität, Bernoullistrasse 32, CH–4056 Basel.

[2]) Tonmineralogisches Labor des Institutes für Grundbau und Bodenmechanik, ETH-Zentrum CH–8092 Zürich.

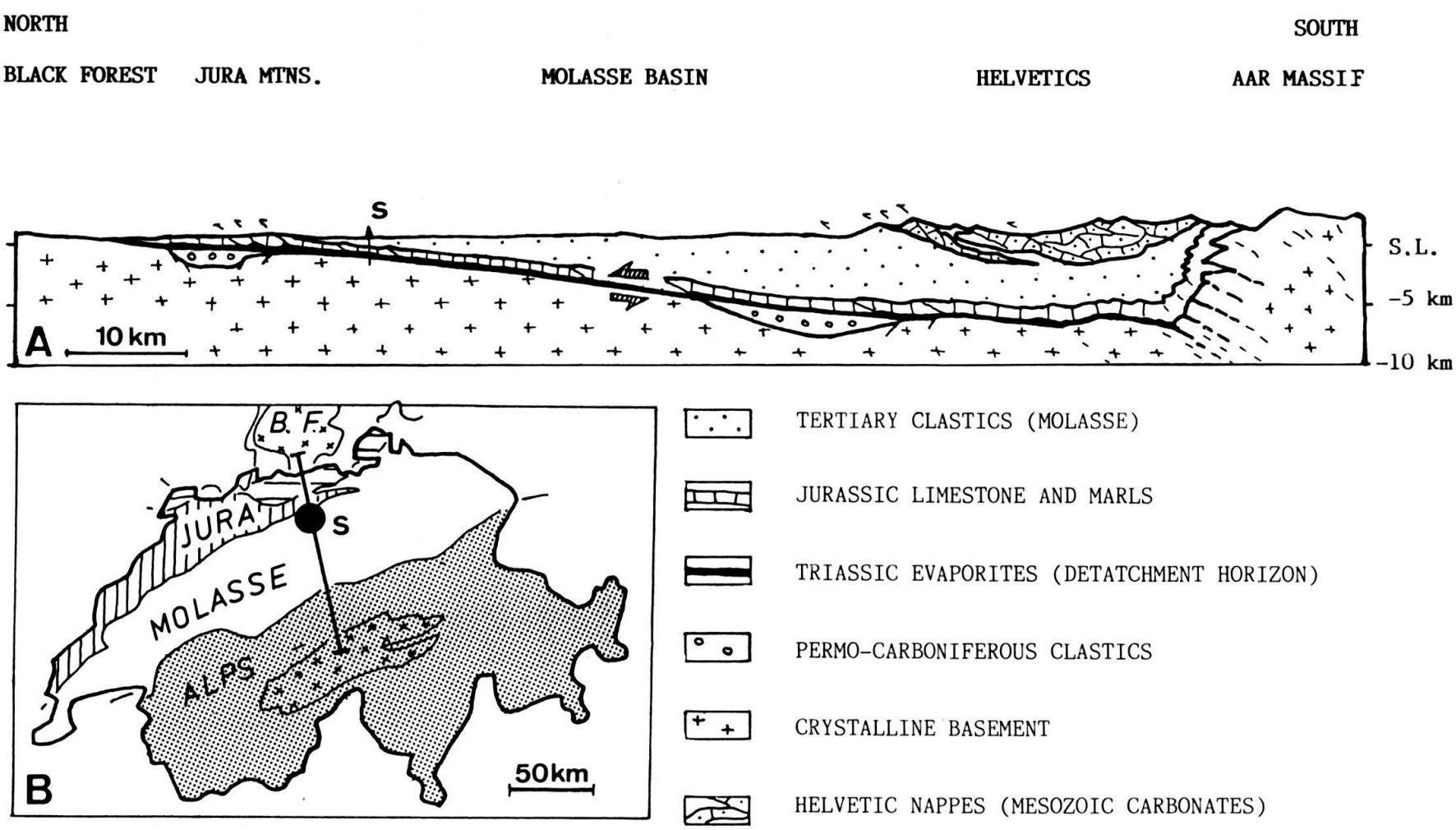

Fig. 1. A. Cross section from the Central Alps to the Alpine foreland through the Schafisheim well ("s", modified after MÜLLER et al. 1984). In this section the movements along the 80 km décollement in the Muschelkalk evaporites amount to 4.5 to 6 km.
B. Location of cross section and Schafisheim well "s").

post Early Triassic sediments and no pre-Middle Triassic sediments are involved in the orogeny, Buxtorf 1907 has suggested that there was a décollement within the Middle Triassic Muschelkalk evaporites ("Anhydritgruppe", Aniso-Ladinian). Buxtorf believed that décollement was localized in the Muschelkalk salt deposits, while Laubscher (1961) has suggested that anhydrites were the detachment horizon because salt occurs too discontinuously to serve as a décollement. Subsequently, strong ductile deformation of anhydrites was found in the Belchen motorway tunnel and the Altishofen well (subordinate detachment in the Late Triassic Keuper evaporites ("Gipskeuper", Carnian): Wohnlich 1967; Laubscher 1975, 1984; Müller et al. 1981, Jordan 1988b), in the Schafisheim well (Müller et al. 1984), and in all other outcrops of the two detachment horizons (e.g. Riepel Quarry AG, Kienberg Quarry SO, Zeglingen Quarry BL, Wiesen well SO; unpubl. work).

Müller et al. (1981) investigated the rheology of anhydrite in experiments and observed a pronounced drop in strenght at high temperatures caused by twinning, intracrystalline glide and dynamic recrystallization by grain boundary migration. At strain rates that are reasonable for Jura overthrusting (1.8 to $13 \cdot 10^{-13}$ s^{-1}), for fine-grained pre-deformed AWP-type anhydrites, the brittle-ductile transition is to be expected above 75–90 °C, i.e. at least 1.6 km of overburden, and for coarser-grained AR-type anhydrites above 110–125 °C (≥ 2.5 km). Assuming deviatoric stresses lower than 50 MPa, the temperature has to have been even higher (ca. + 25 °C for AWP-type, and ca. + 60 °C for AR-type, respectively) to result in the strain rates outlined above. These experimental data explain the ductile flow of anhydrites for most of the detachment horizon (Müller & Hsü 1980), but do not fully explain the ductile flow anhydrite within the more shallow parts of the overthrust, e.g. Schafisheim well with its original overburden of less than 1.8 km (Jordan 1987b), Belchen motorway tunnel (1.5 km, Laubscher 1984, Jordan 1988b). Therefore, some geologists have suggested other mechanisms for ductile flow of anhydrite, such as pressure solution, diffusion in aqueous films along grain boundaries and precipitation as semistable bassanite or gypsum that acts as a lubricant (Laubscher, 1984).

The purpose of this paper is to describe some typical deformation structures found within the Muschelkalk evaporites of the Schafisheim well, and to discuss the role of anhydrite during Jura overthrusting.

The Muschelkalk evaporites of Schafisheim

Tectonical and geophysical setting

At Schafisheim well, drilled by the Swiss National Association for Radioactive Waste Disposal (Nagra), and located in the hinterland of the Jura (Fig. 1), the Muschelkalk evaporites were completely recovered. These evaporites are believed to have absorbed almost all of the detachment movement, which, in this area, amounts to some 4.5 to 6 km according to different interpretations of outcrop and seismic data (e.g. Jordan 1987b). The Muschelkalk evaporites were found at a depth of 1357 to 1435 m (Weber et al. 1986). The present temperature at this depth is 61 to 64 °C according to a geothermal gradient calculated by Diebold & Müller (1985). Direct measurements within the borehole-fluid yielded somewhat lower temperatures (51 to 53 °C, Weber et

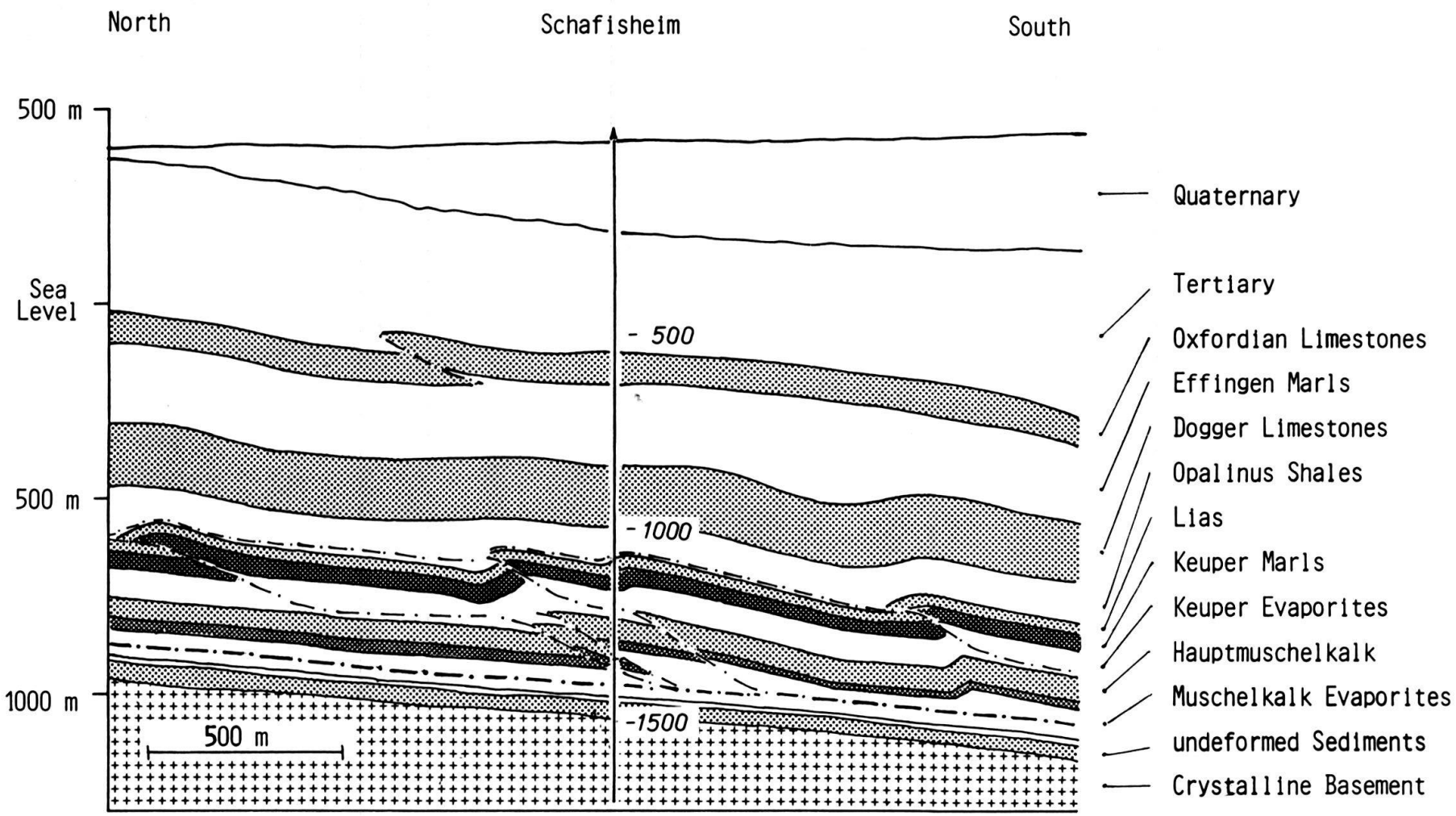

Fig. 2. Main litho-rheological units encountered in the Schafisheim well. The cross section shows a probable interpretation of the core (Weber et al. 1986) and seismic data (Sprecher & Müller 1986). The strike direction changes from E-W in the upper sequence (above subordinated thrust at 1320 m) to SSE-NNW (between this thrust and the main detachment horizon at ca. 1430 m) and finally to ENE-WSW in the footwall.

al. 1986). The paleotemperature during the overthrusting is believed to have ranged between 70 and 78 °C based on today's geothermal gradient and on a reconstruction of the original overburden (1.8 km, NAEF et al. 1985, cf. JORDAN 1987b).

The cross section through the Schafisheim well (Fig. 2) displays some imbrications of the competent carbonate layers between the less competent evaporite and shale layers. These imbrications were caused by small thrusts which interconnected the main décollement within the Muschelkalk evaporites with subordinate décollements within the Keuper evaporites and the Opalinus shales (MÜLLER et al. 1987). One of this thrusts which doubled the uppermost 15 m of the Muschelkalk evaporites was encountered at 1320 m Figs. 2 and 3).

Stratigraphy

Compared to the unsheared foreland sequences, the Schafisheim anhydrite strata have hardly been thinned (DRONKERT 1987). Some of the Schafisheim horizons have even been thickened by folding. The most prominent difference between these sequences is the occurrence of a salt layer (IV and V in Fig. 3) that is three to six times thicker than corresponding members in the foreland.

The Muschelkalk evaporites are overlain by the Ladinian crinoidial Limestones of "Hauptmuschelkalk". DRONKERT et al. (1989) subdivide the Muschelkalk evaporites ("Anhydritgruppe") into six members (Fig. 3): The predominantly dolomitic and sulphate-silica-bearing layers of the "Dolomit der Anhydritgruppe" (I) form the top of the sequence (beginning at 1287.1 m in the upper thrust sheet). Near the bottom of member I, dolomite is interlayered with anhydrite. This interlayering continues into the top part of the "carbonate-rich sulpharenites" (II). The sulpharenites are underlain by the dark thin-layered "sulpharenites-selenites" (IIIa) and the "layered sulpharenites" (IIIb). Member I to III correlate in thickness and lithology with sequences of the undeformed foreland. Member III overlays 45.2 m of coarse-grained rocksalt subdivided by anhydrite beds and lenses of various size which become rare in the lowermost part. DRONKERT et al. (1989) combined this sequence as "salt layers" (IV & V) and suggest a correlation with the members "sulphate/carbonate breccias" (IVa), "lower layered sulpharenites" (IVb) and "salt layers" (V) of the undisturbed foreland. The most spectacular anhydrite interlayer, a nearly perpendicular double-fold between 1393.4 to 1400.7 m below surface, may be correlated with member IVb.

The lower sulphate layers form the lowermost member of the Muschelkalk evaporites (VI). They are underlain by the Lower Muschelkalk carbonates ("Wellengebirge", 36 m) and the sulphate-bearing Buntsandstein siliclastica (Lower Germanic Triassic, Skythian, 2m). The Buntsandstein directly overlies the crystalline basement.

Extent of present investigations

To estimate the strain suffered by the Muschelkalk evaporite and to locate horizons that accommodated major shear movements, the whole evaporite sequence was inspected directly and in color photographs. We then sampled eigth core sections of approx. 20 cm in length each (Fig. 4). The eight core samples were cut normal to local strike, polished and etched with formic acid to enhance the small scale structures. The

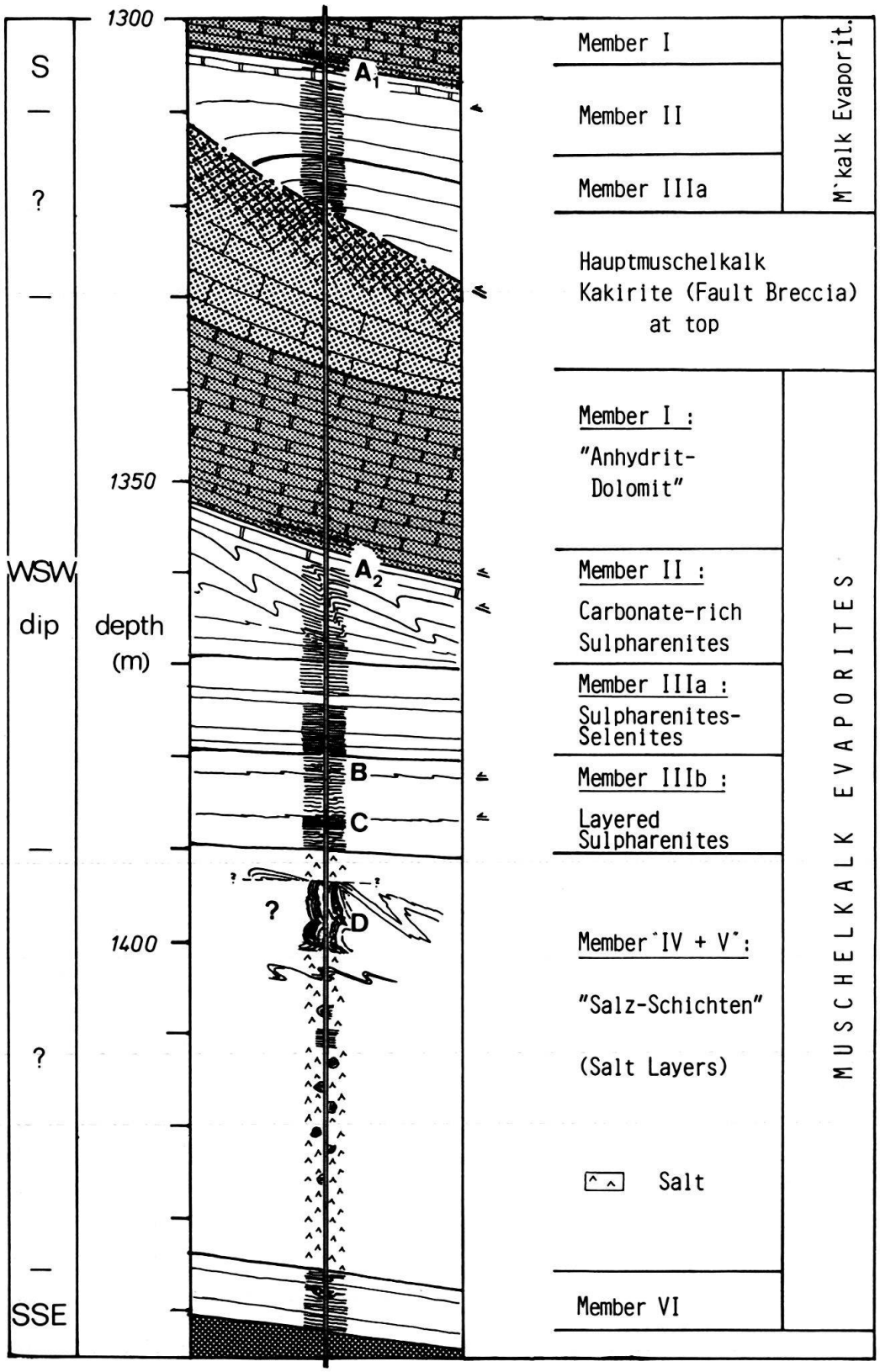

Fig. 3. Stratigraphy and structures of Muschelkalk evaporites ("Anhydrit-Gruppe") from Schafisheim based on data from Dronkert (1987), Dronkert et al. (1989), and Weber et al. (1986). Structures within the core (double line in center) are extrapolated to both sides. Interfaces of members are marked by heavy lines, stratigraphic column refers to depth of interfaces within core section. Letters A to D refer to detailed sections shown in Fig. 4.

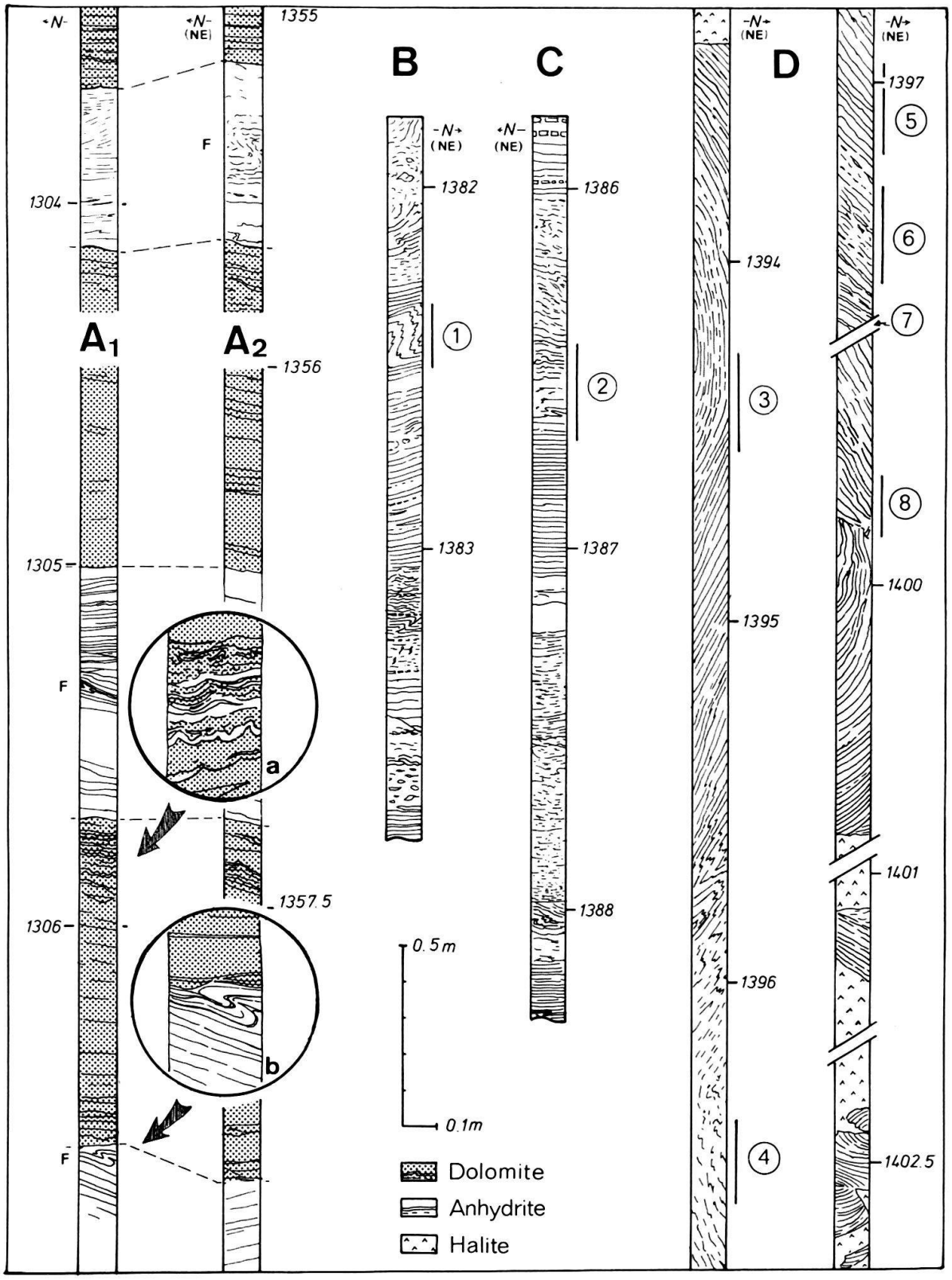

Fig. 4. Selected core sequences from Muschelkalk anhydrite showing details of tectonic structures. For location see Fig. 3. In this and the following figures, depth is below surface. Numbers 1 to 8 refer to core samples. North is believed to be on the left for sequences A and C, and on the right for sequences B and D (see text). The magnifications of sequence A_1 show sedimentary (a) and tectonic folding (b).

true orientation of the cores is not known. Stratigraphic high resolution (SHRT) and Sonic televiewer (SABIS) logs (WEBER et al. 1986) as well as tectonic considerations were used to orient the cores. Ultra thin sections were then prepared from domains with very promising deformation structures. Regular thin sections from other domains, originally sampled for sedimentological reasons (DRONKERT et al. 1989), served as a reference for the discrimination of tectonic from sedimentary and diagenetic structures.

The mineralogy of some layers which showed different rheological behavior was investigated by X-ray diffraction (Table 1). Since some layers are only a few mm thick, the material from the layers was excavated with a dental drill. An alcohol-sediment suspension was transferred by pipette to a glass slide and dried at room temperature. Alcohol was used instead of distilled water to prevent the alteration of anhydrite to gypsum (gypsification). All specimens were X-rayed at 40kV, 30mA, 120s/deg with a PW 1700 automated powder diffractometer.

Deformation of the Muschelkalk avaporites

Members I to IIIa

The most conspicuous tectonic structure at Schafisheim is the doubling of the uppermost Muschelkalk evaporites by thrusting at 1320 m Fig. 3). Thrusting was accompanied by strong brecciation of the Hauptmuschelkalk limestones of the footwall. The sulpharenites-selenites (IIIa) of the hanging wall form a gentle drag fold with practically no brittle deformation structures. Although nearly undeformed in the upper part of member IIIa, the sedimentary structures are increasingly flattened towards the thrust by ductile shear.

Internally, the upper thrust sheet is nearly undeformed except near the interlayered transition between member I and II (Fig. 4, A_1). Asymmetric to isoclinal layer-parallel folds are developed at the top of some anhydrite layers, e.g. at 1306.65 m (Fig. 4b). These flow folds resulted from the concentration of shear at the position of maximum competence contrast between the brittle dolomite, and the ductile anhydrite which underlies it. The axial planes of the folds indicates a north-ward (sinistral in Fig. 4b) movement implying that these structures are the result of Jura overthrusting. Furthermore, similar folds were found in the same stratigraphic position in the lower thrust sheet at 1355.4 m (Fig. 4, A_2) suggesting that décollement predated the local doubling of the strata.

Although only sligthly deformed in the upper thrust sheet, the carbonate-rich sulpharenites (II) of the lower thrust sheet are bent into spectacular asymmetric folds (Fig. 3). The folds formed in a ductile manner, initially, but were later overprinted in a brittle regime as documented by brecciated flow structures. As a result of the folding, member II of the lower thrust sheet is 3.2 m or 32% thicker than member II of the upper thrust sheet (apparent thickness, DRONKERT et al. 1989).

Within the "sulpharenites-selenites" (IIIa) of the lower thrust sheet, the downward-increasing flattening of the sedimentary structures is even more pronounced. The flattening is pervasive in the salt-bearing sequence between the prominent "selenitic marker bed" (SM in Fig. 3) and member IIIb.

core	layer	anhydrite	gypsum	magnesite	dolomite	calcite	halite	quartz	clay min.
1	1-3	84	4		7			5	
	1	70	5		17			8	
	2	75	6		11			8	
	3	95						5	
2	4-10	91	4		3			2	
	4	75	5		20				
	5	95			5				
	6	87	8		5				
	7	98	2						
	8	95	5						
	9	93	7						
	10	87	6		4			3	
3	1	50	6	40				2	2
	2	93	3					4	
6	I(A-E)	91			4			5	
	II(F-L)	88			5			7	
	III(F)	95			3			2	
	(A-F)	92			4			4	
	A	85			5			8	2
	B	95			3	2		5	
	C	40			20	5	10	10	15
	D	82			8	5		5	
	E	85			10			5	
	F	90			5			5	
	G	95			2			3	
	H	60	5		15			10	10
	K	5	10				85		
	L	82	6			2		10	

Table 1. Mineralogical composition of some selected layers of core samples 1, 2, 3 and 6 (Figs. 5, 8, 11 and 14, respectively). Contents in volume percent.

Member IIIb

From a rheological point of view, the "layered sulpharenites" (IIIb) are the most interesting part of the Schafisheim sequence (B and C in Fig. 4). In contrast to corresponding sequences from the foreland, the Schafisheim sequence is strongly tectonized. Major shear movements are displayed by a strong overprint of original sedimentary structures and by spectacular layer-parallel asymmetric and even isoclinal ductile folds. The deformation is not pervasive but limited to distinct horizons. The varying lithologies and their different theologies has resulted in nearly undeformed sedimentary structures in the immediate vicinity of strongly sheared rocks.

Core sample 1 shows one of these asymmetric folds from the upper part of the layered sulpharenites (Fig. 5). Although this fold probably originated as a sedimentary fold or undulation, it has been tectonically enhanced and overprinted. The near-vertical short limb has been thickened compared to the horizontal long limbs. The fold formed within a nearly pure anhydrite with graded dolomitic interlayers (increasingly ligther grey, up to 17% fine-grained dolomite and 8% quartz, Table 1). With increasing content of brittle components (dolomite and quartz), the layers become brittle themselves. A beautiful example of the different ductilities of differing horizons is shown on

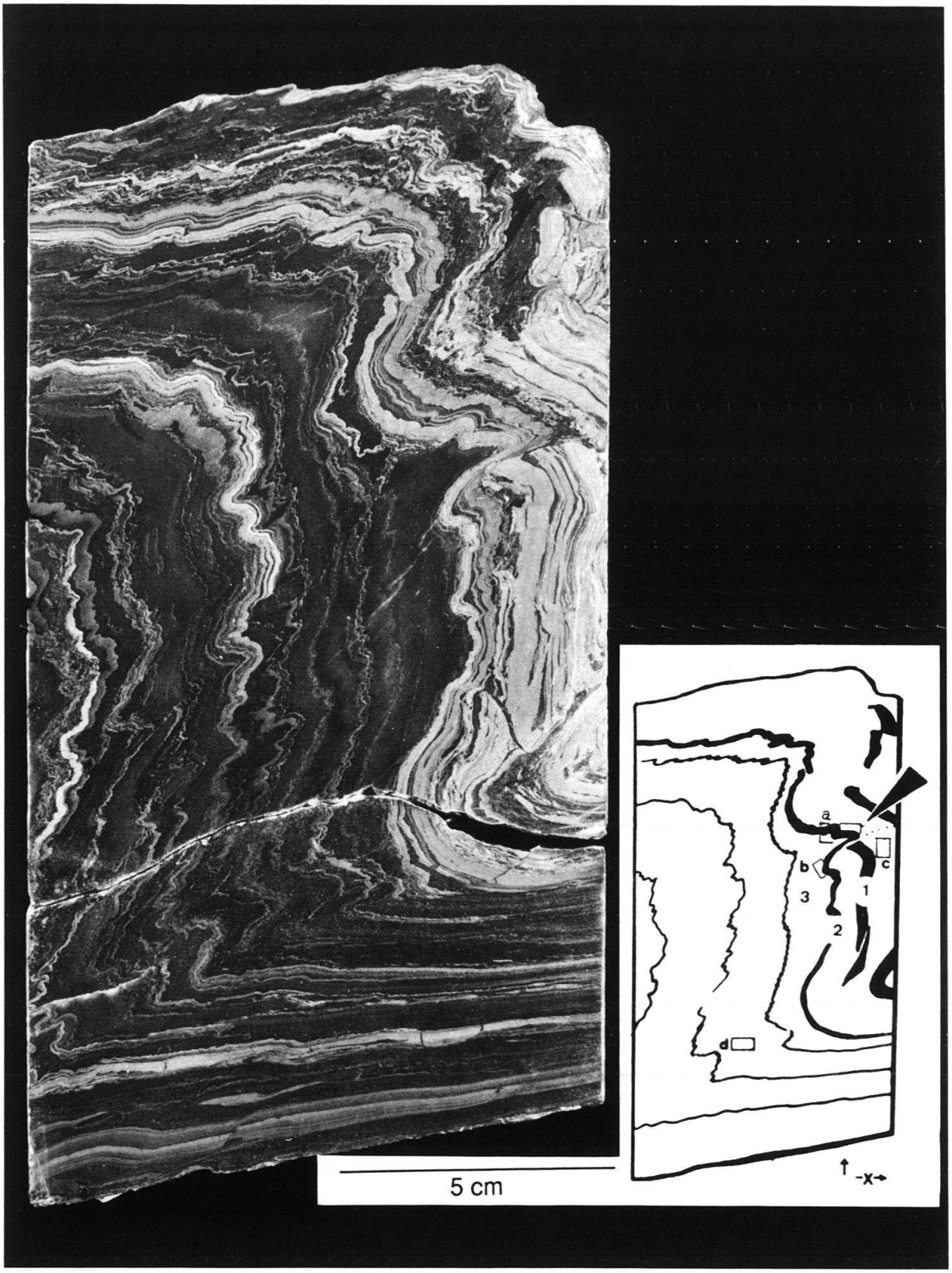

Fig. 5. Core sample 1 (1382.32–1382.50 m, upper part of member IIIb). The core was cut perpendicular to local strike direction. The surface is polished and specially treated in order to distinguish pure anhydrite (black) from dolomitic layers (increasingly lighter grey). Numbers of inset refers to Table 1, and letters to Fig. 6. Notice the different rheological behavior of the various lithologies.

Fig. 5. The almost pure anhydrite (layer 3) is ductile and incompetent. The next two layers to the right are still ductile but more competent (e.g. layer 2). Layer 1 is most competent and is intersected several times by brittle shear zones. On an enlarged scale, the variations in mechanical behavior are clearly visible in a graded bundle of graded sequences (Fig. 6c). The anhydritic dolomite sequences at bottom behave brittly, the dolomitic anhydrite sequences in the middle are kinked, while the nearly pure anhydrite sequences at the top are gently folded. Furhermore, there are some noteworthy differences in the deformational behavior of anhydrite in pure and dolomitic sequences. In the pure anhydrite the elongation and lattice preferred orientation of anhydrite grains run parallel to the axial plane of the fold (Figs. 6a and b), while, within the dolomitic layers, elongation and lattice preferred orientation of anhydrite grains run parallel to layering and are bent around folds and kinks (Figs. 6a and c). High competence contrast between pure and dolomitic anhydrite is indicated by a characteristic cleavage pattern in the pure anhydrite indicative of negligible shortening parallel to the axial plane in the dolomitic layer (Fig. 6d).

Within *Core sample 2* (Fig. 7), folds of various shapes and origins were found. From top to bottom, a continuous transition from well preserved sedimentary structures to strongly sheared pure anhydrite forming recumbent and layer-parallel isoclinal folds may be observed. The box-fold like structures in the upper part of the sample are believed to be of sedimentary to diagenetic origin. Similar structures are found in tectonically undisturbed sediments of the foreland. Just above layer 8, sedimentary structures are distinctly tectonically overprinted. The structures of the lower half of the sample are definitely of tectonical origin as documented both by the geometry of the folds and by structural evidence.

The recumbent shear folds, outlined by layers with some dolomitic impurities (up to 5%, Table 1, layers 5, 6 and 10) show a distinct and pervasive axial plane parallel cleavage (Fig. 8a). In the pure anhydrite layers (e.g. Fig. 8b), a pronounced texture suggests a strong extension in E-W direction, but the anhydrite grains are only slightly elongated. Based on some similarities to patterns in deformed limestone mylonites (e.g. Schmid 1982), we denote this structure as mylonite-like (see discussion below).

The strain documented in this section is difficult to estimate. Some of the very thin layers which have higher dolomite contents (e.g. layer 4, 20%) form parasitic parallel folds with very short wavelengths and high amplitudes (cf. Fig. 6d). Assuming that there was hardly any layer parallel shortening, dolomitic layer 4 yields a minimum value of 40% shortening (between visible end points) which results in a shear value γ of approx. 3 for this sequence. We believe that the shear strain within the underlaying pure anhydrite with mylonite-like structure is significantly higher.

Member IV and V

These sequences are characterized by strongly tectonized anhydrite layers which are separated by rocksalt intervals of differing lengths. The succession IVa-IVb-V as found throughout the whole foreland is completely disturbed at Schafisheim.
A spectacular double fold was discovered between 1393.4 m and 1400.7 m (Fig. 3 and D in Fig. 4). It is localized in the uppermost part of the "salt layers" (member IV and V) and is separated by about 3 m of rocksalt from the strongly sheared layered sulpharenites above. The double fold includes a nearly perpendicular, gently bent upper fold,

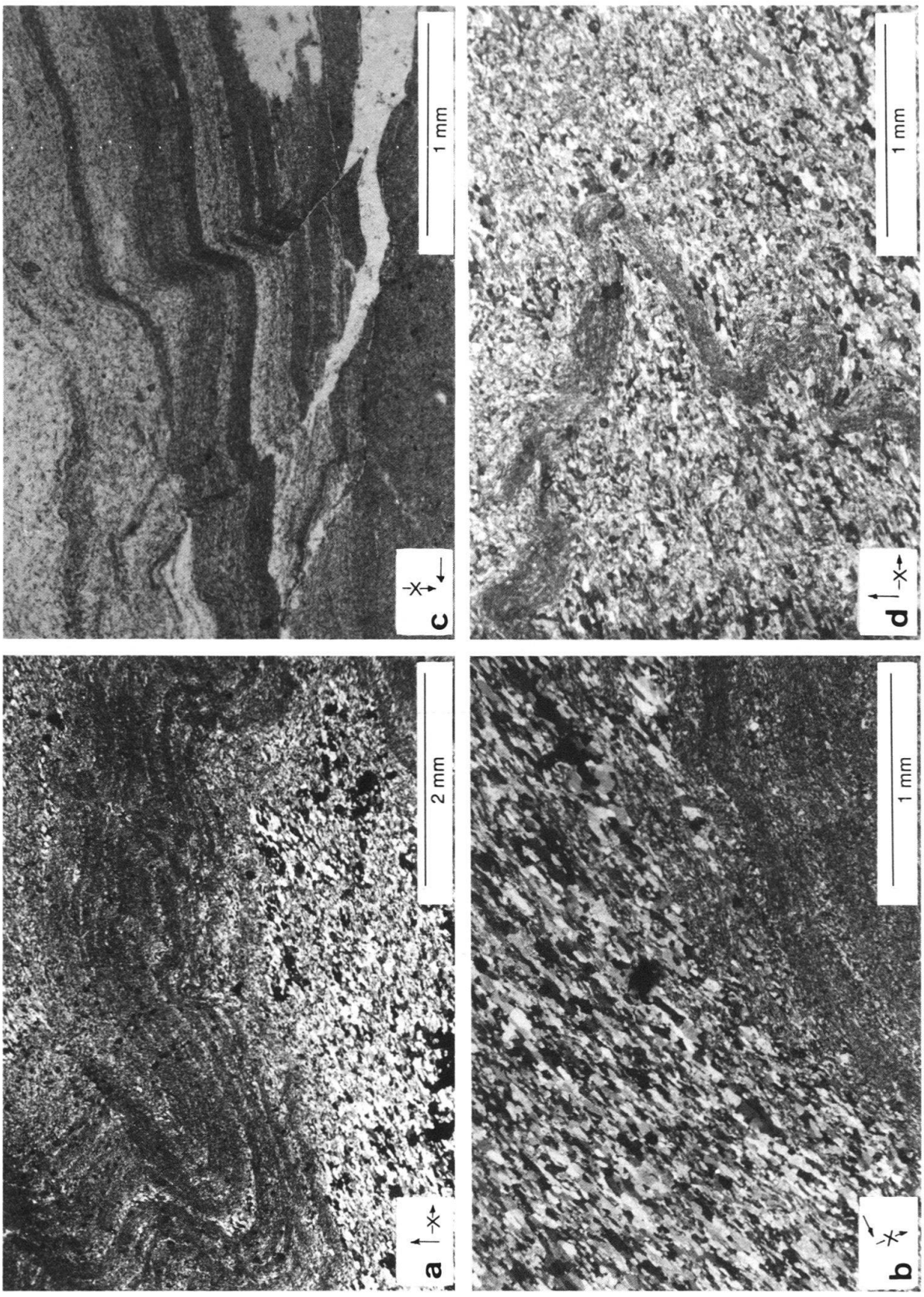
a
2 mm
b
1 mm
c
1 mm
d
1 mm

a complex isoclinally folded interconnecting hinge, and a lower open fold with a very sharply-bent kink-like hinge. The layering of the beds is cut at both ends, and it is unclear whether it is a continuous anhydrite bed or a mega-clast within the rocksalt. This fold is probably part of the (lower) "layered sulpharenites" (IVb, DRONKERT 1987), which were first folded and later dismembered.

Core sample 3 (Fig. 9) shows an upright sequence of pure anhydrites rhythmically grading upwards (to the right) into magnesitic anhydrites (e.g. layer 2 into layer 1, Table 1). A distinct conjugate shear system documents a layer-parallel stretching (Fig. 9b). This brittle system affects only the more competent magnesitic layers to the right of layer 2 and fades away in this ductile pure anhydrite layer. Ductile deformation is also found in all other pure anhydrite interlayers to the right. The magnesitic horizons are boudinaged and some of them were later imbricated (e.g. layer 1 in upper part of Fig. 9 and in Fig. 10). Similar layer-parallel stretching by symmetric conjugate shear systems is also common in upright fold limbs and thrust sheets within the subordinate Keuper evaporite detachment horizon of the Belchen Motorway tunnel (JORDAN 1988b). Therefore, we believe that in core sample 3, this stretching also postdates the upright rotation and documents a late subhorizontal constriction of the folded sequence. On the other hand, some boudinage and the imbrication of these boudins are probably related to earlier stages of folding.

Core sample 4 (1396.39–1396.62 m, not figured) originates from the interconnecting hinge of the double fold and shows a multilayer of anhydrites grading into magnesitic anhydrites. The multilayer is strongly folded in small scale parasitic folds. The magnesitic interlayers were first boudinaged and later strongly imbricated.

Core sample 5 (1396.95–1397.20 m, not figured) shows strong layer-parallel extension of anhydrites with some few thin boudinaged magnesitic interlayers. No imbrication may be observed.

Core sample 6 (Fig. 11a, d) shows the differing rheological behavior of the various lithologies. Beside anhydrite, magnesite and quartz, clay and rocksalt are involved (Table 1). The most competent layers are the marly anhydrites C and H, which are often boudinaged and imbricated in parts. Both are embedded in nearly pure ductile anhydrite; layer C (40% anhydrite) which forms barrel-shaped boudins is distinctly more competent than layer H (60% anhydrite) which has a pinch and swell structure. The rocksalt of layer C is restricted to joint fillings. The rocksalt between layers E and G (black in Fig. 11a), is believed to have originally formed idiotopic cubes as they are still found in less deformed foreland samples (Fig. 11b, Widmer 1989). The cubes have been squeezed into a typical cuspate-lobate form in the way described recently on the basis of deformation experiments on halite cubes in a more competent matrix (Fig. 11c, JORDAN 1987a). Obviously, rocksalt was less competent than the surrounding anhydrite.

Fig. 6. Micrographs from core section 1 (crossed nicols), for location see Fig. 5 (b and c are rotated mirror images in respect to Fig. 5, see orientation marks):

a) Layers 3 and 2 in the hanging wall of the most prominent thrust in Fig. 5 (arrow). Note kink-like drag folds in layer 2.

b) Strong elongation of grains parallel to fold axis within pure anhydrite layer 3, layer 2 is visible at bottom.

c) Differing rheological behavior with increasing carbonate content. From top to bottom: flow folds in nearly pure anhydrite, kink-like folds, kink, and finally anhydrite-filled joints in brittle anhydritic dolomite.

d) Parallel fold of thin dolomitic layer within pure anhydrite of much lower competence.

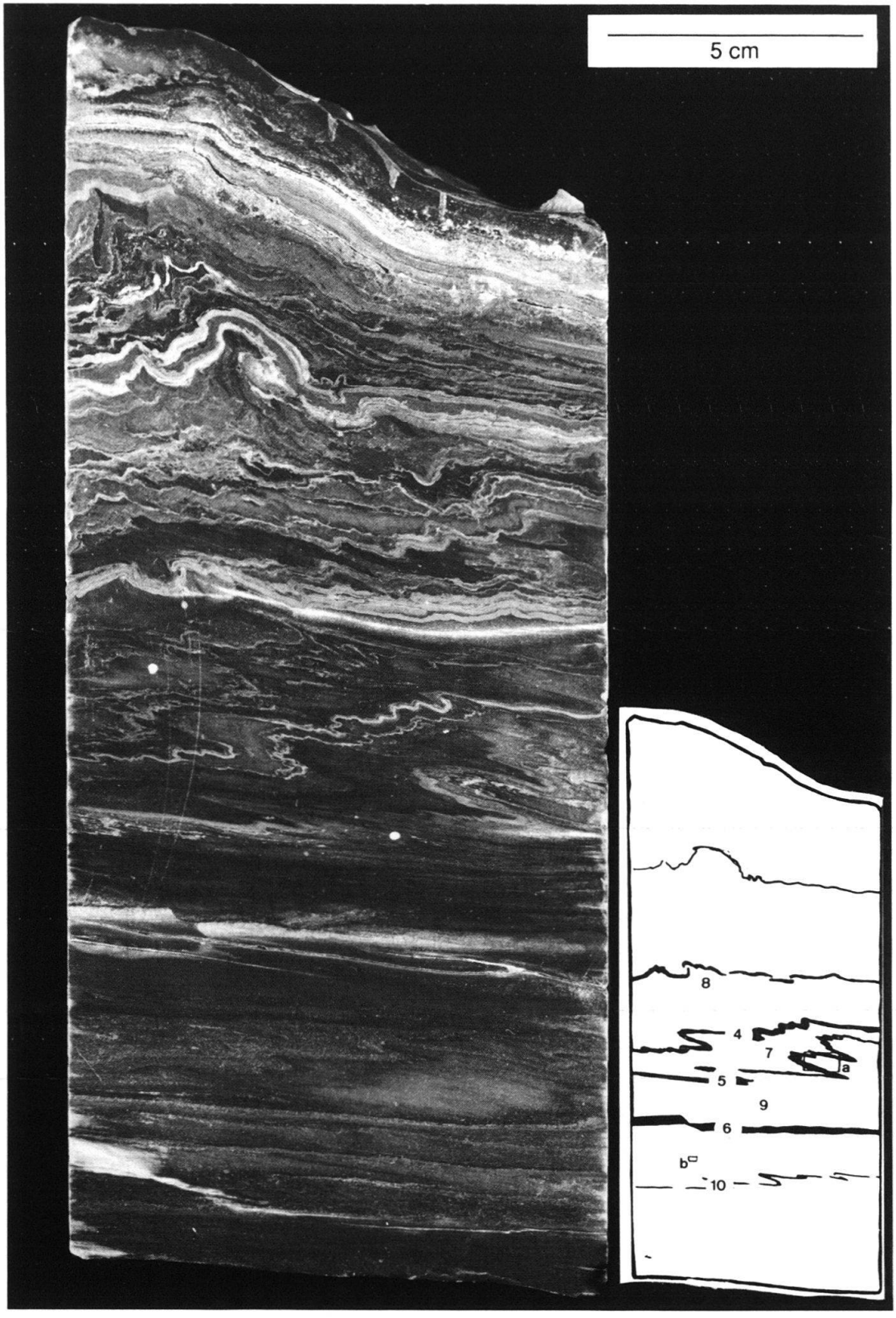

Fig. 7. Core sample 2 (1386.43–1386.70 m, lower part of member IIIb). For general informations cf. Fig. 5. Strain documented in folding becomes stronger from top to bottom of sample. Notice recumbent isoclinal folds in center.

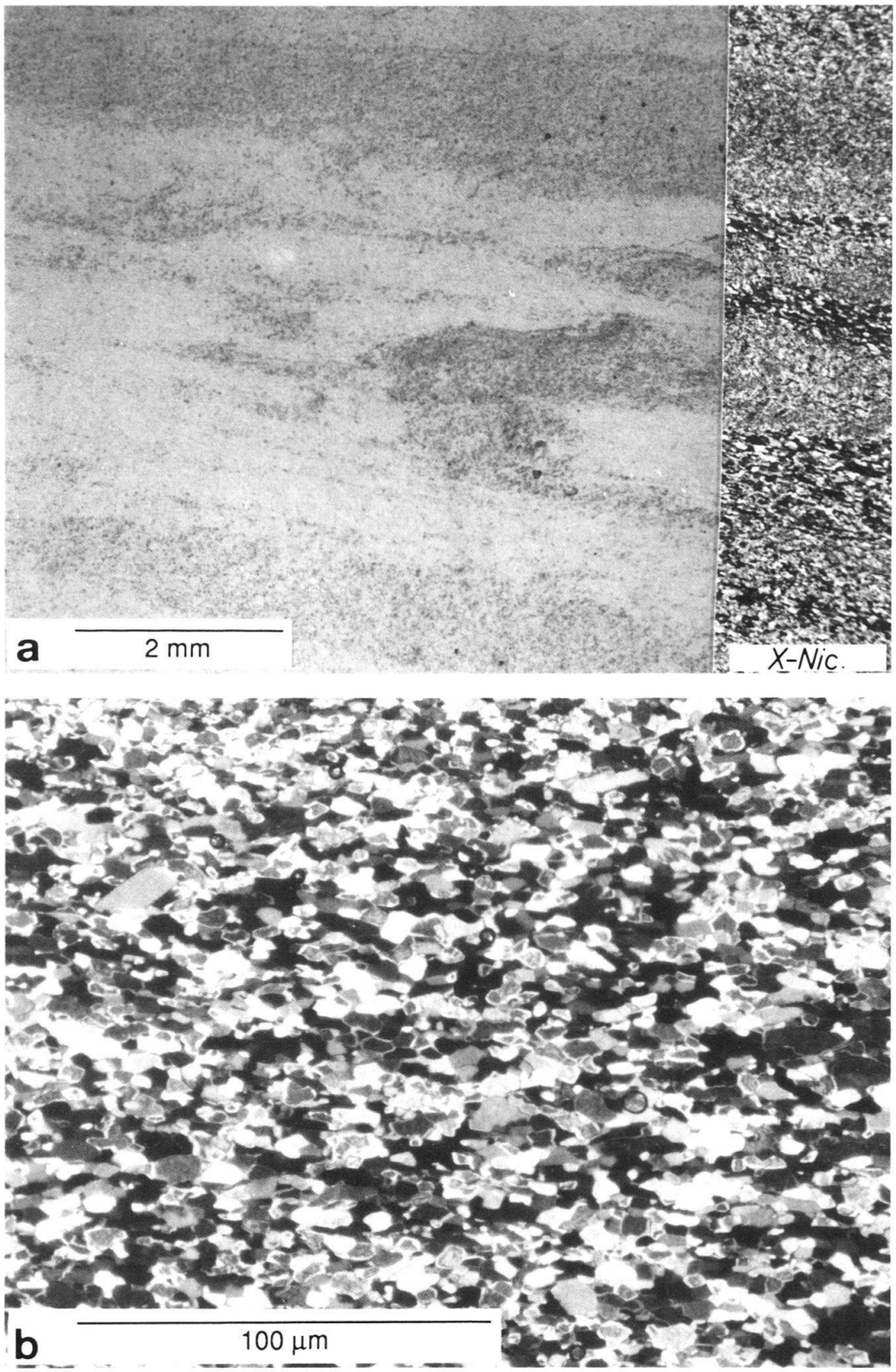

Fig. 8. Micrograph from core sample 2, for location see Fig. 7.
a) Core of the isoclinal recumbent fold. In plan light, dolomite impurities are visible (ieft), continuation to the right under crossed nicols.
b) Mylonite-like fabric within pure anhydrite. Crossed nicols.

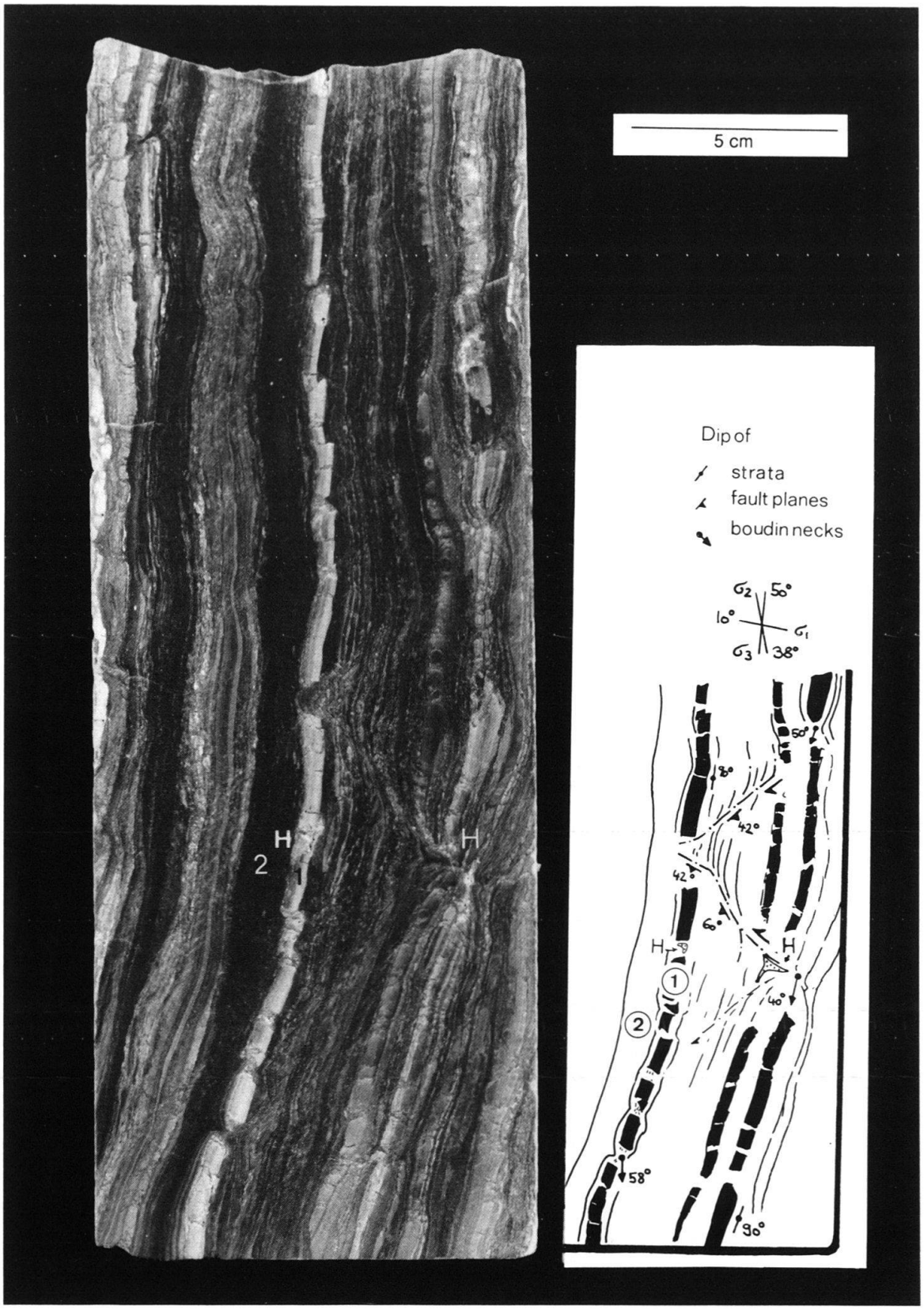

Fig. 9. a). Core sample 3 (1394.26–1394.53 m upper hinge zone of the upright double-fold within the "salt layer"). b) Sketch of tectonic structures of the lower right part of the core showing a late horizontal shortening perpendicular to layering. Dip values refer to cut surface. Orientations of principal stress directions result from analysis of horst-graben structures (σ_1 is maximum compression). Numbers refer to Table 1 and micrographs.

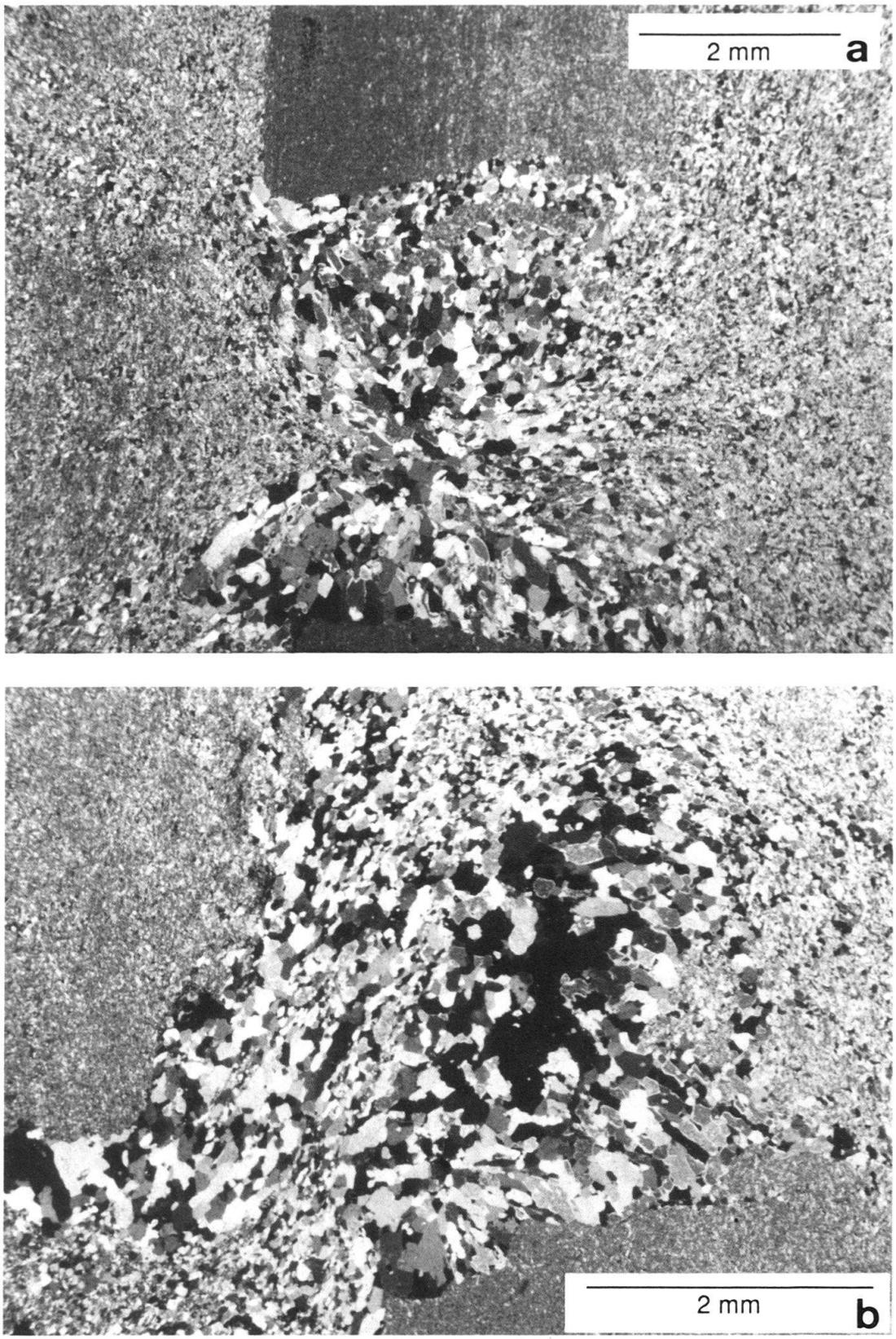

Fig. 10. Micrographs showing simple and imbricated boudinage of layer 1 in Fig. 9 (crossed nicols). The microstructure of the pure anhydrite boudin necks is altered by postkinematic static recrystallization.
a) Boudin neck in extension with barrel to fish mouth form. Notice strong flow of incompetent anhydrite into boudin neck.
b) Overthrusted boudins. Notice strong elongation of grains parallel to shear in former extension vein.

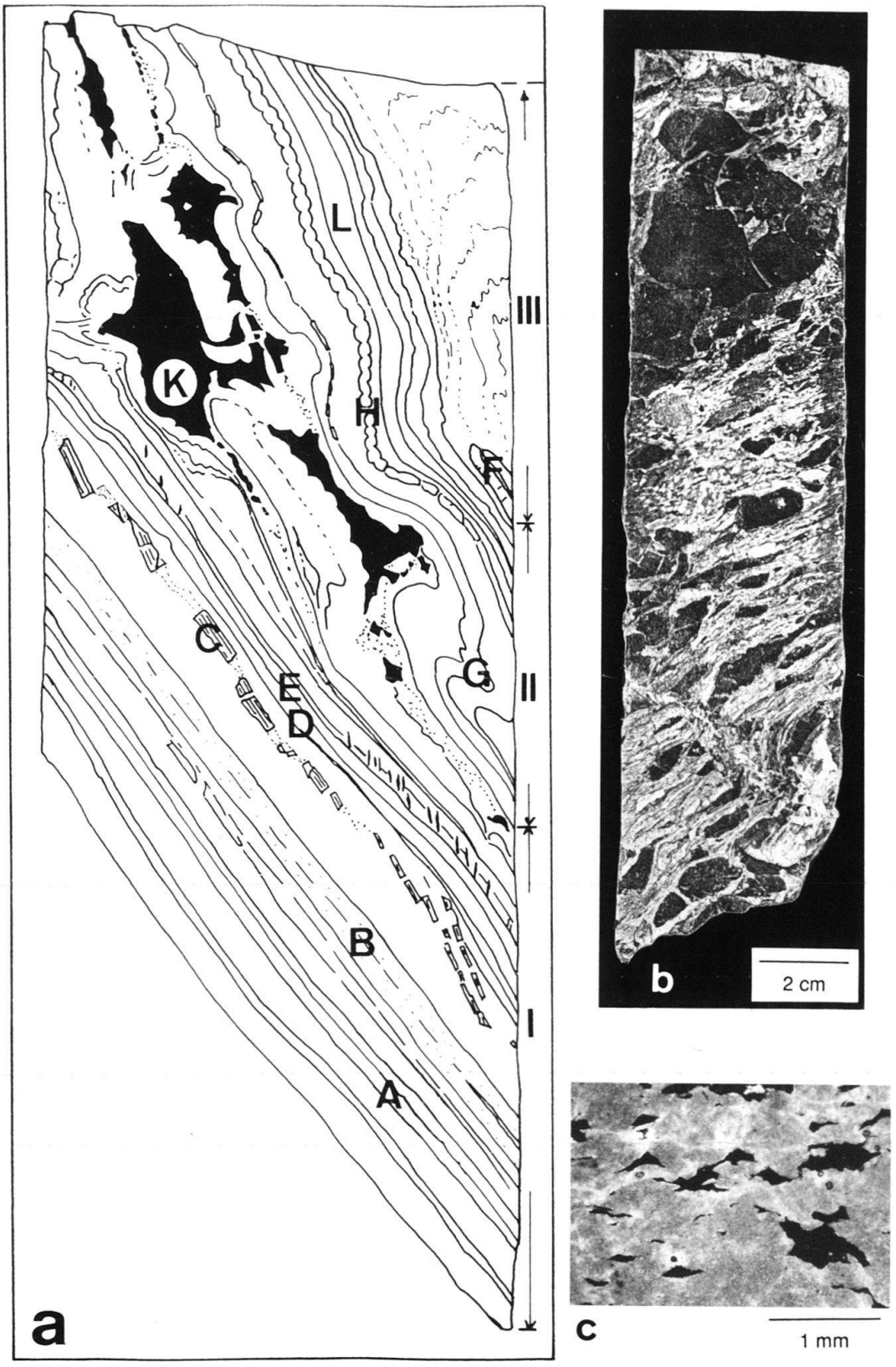

Fig. 11. a) Sketch of core sample 6 (cf. d), halite is black, letters refer to Table 1.
b) Less deformed halite idioblasts within a mainly anhydritic sequence of Hauptmuschelkalk evaporites (Adlerhof Anticline, Tabular Jura, section provided by Th. Widmer).
c) Experimentally deformed halite idioblasts in limestone matrix showing typical cuspate-lobate grain boundaries (σ_1-direction is vertical, from Jordan 1987a).

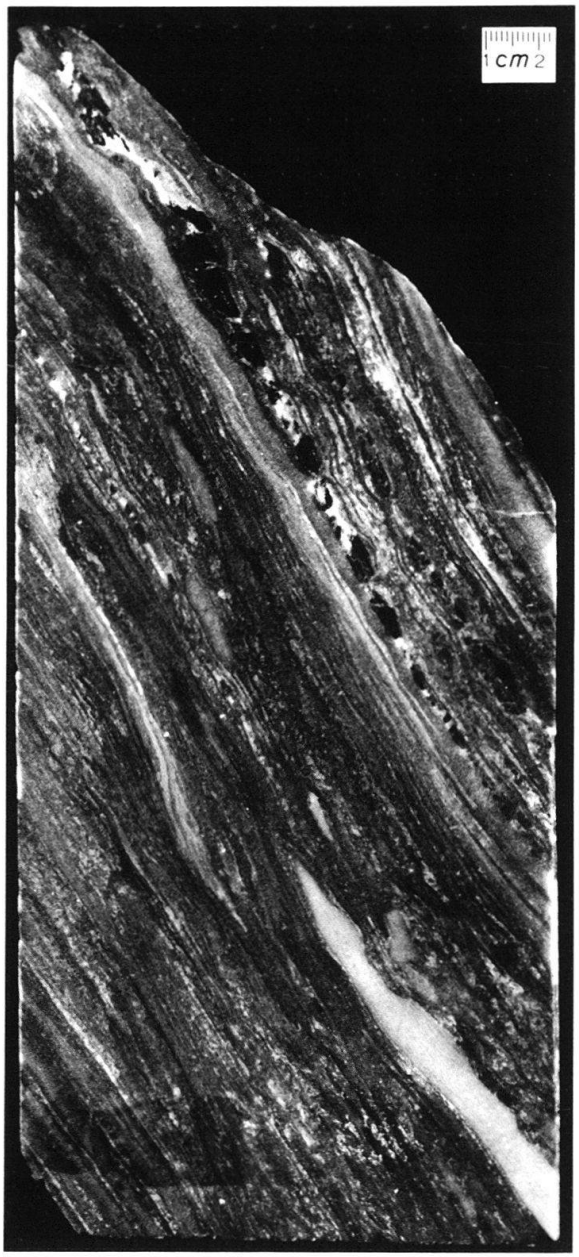

Fig. 11.d) (left). Core sample 6 (1397.30–1397.58 m, upper limb of lower fold). Notice differing rheological behavior of various lithologies.

Fig. 12. (right). Core sample 7 (1396.39–1396.62 m, upper limb of lower fold) with stretched anhydrite nodules (pale, bottom right).

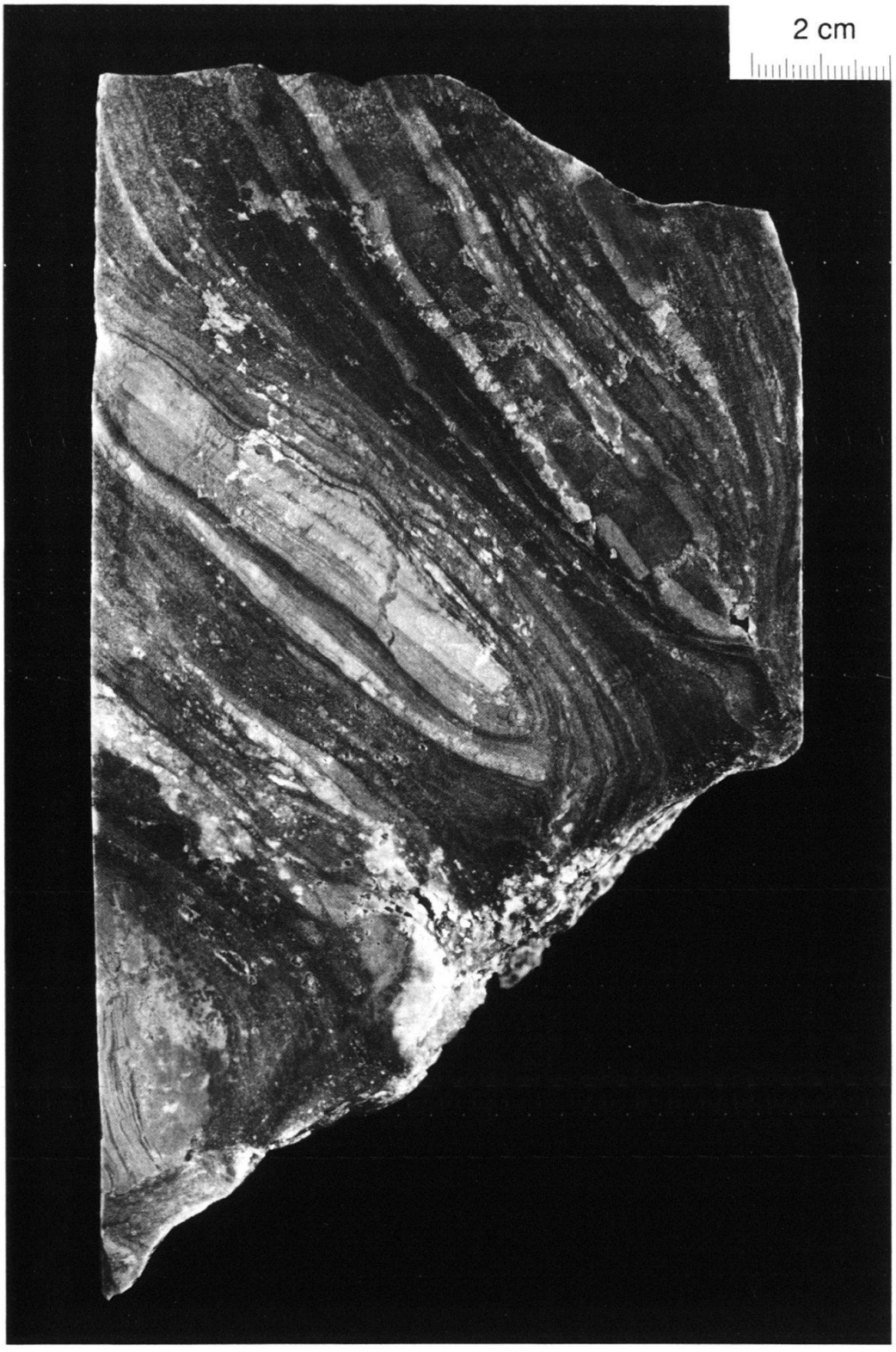

Fig. 13. Core sample 8 (1399.70–1399.87 m). Boudinage within the upper part of very sharp hinge of lower fold.

Core sample 7 (Fig. 12) shows an anhydrite with strong layer-parallel extension. Correspondingly to core sections 3, 5, and 6, magnesitic layers are boudinaged. Here, no imbrication may be observed. Noteworthy are the pink anhydrite lenses (pale in Fig. 12), which are believed to be stretched anhydrite nodules.

Core samples 8 (Fig. 13) shows complexe boudinage of magnesitic layers of various magnesite contents. The high-magnesite layers in the core of the larger boudins are barrel shaped, while the surrounding and less competent layers form a pinch and swell structure. Rupture within the inner layers is fully compensated by ductile flow of the outer layers and the dark pure anhydrite. Core sample 8 is the hanging wall part of the very sharp hinge of the lower fold. The bottom surface of the sample is identical to the axial surface of this fold.

Beside the double fold, folded anhydrite clasts and beds are also found in the lower, halite-dominated part of member IV and V (e.g. Fig. 4, D, 1402.5 m). These clasts are believed to be relicts of dismembered folds suggesting that the rocksalt layer is strongly sheared.

Member VI and the underlaying formations

These sequences are only slightly deformed. The anhydrites of the lower sulphate layers (member IV) show some ductile deformation. The carbonate "Wellengebirge" and the mostly sulphate-bearing siliciclastic Buntsandstein suffered a slight and insignificant cataclastic deformation as documented in veins of Jura-overthrust age (Ramseyer 1987).

Partitioning of strain by the different members

Internally, the predominantly brittle "Anhydritdolomit" (I) is nearly undeformed. Only small shear deformations have been recorded from the "carbonate-rich sulpharenites" (II) and the "lower sulphate layers" (VI). We suggest that the total shear accommodated by these formations amount to a maximum of 500 m. But, the Muschelkalk evaporites have been sheared over 4 to 6 km in the Schafisheim area (e.g. Jordan 1987b). Therefore, we suggest that the members III to V and the interface between members I and II accommodated the additional 4 to 5.6 km of shear movements. These members have a total thickness of 71 m. Consequently, the shear strain γ would range between 57 and 80. Based on the assumption that the Jura overthrusting was active for 2 to 10 million years (Laubscher 1980; Naef et al. 1985) strain rates between $1.3 \cdot 10^{-12}\ s^{-1}$ and $1.8 \cdot 10^{-13}\ s^{-1}$ are suggested.

Some aspects of deformation in anhydrites

Sedimentary and diagenetic versus tectonic folding

Folds of all scales in sulphate rocks are often described and interpreted to be of tectonic origin (e.g. Buxtorf 1907, Wohnlich 1967, Laubscher 1975, Borns 1983, Baumann 1984 etc.). Folds in evaporites, however, may originate by tectonism, diagenesis or even sedimentation. In the sedimentary environment folding may be produced by slumping, loading, convolution of a bed, algal growth, differential desiccation, or ex-

cessive crystal growth. ("enterolithic folds", cf. DRONKERT et al. 1989). During diagenesis, gypsification, anhydritization, dolomitization, and dissolution of salts ("subrosion") may cause folding and faulting. Finally, the dehydration of gypsum into anhydrite (or vice versa) may also produce enterolithic folds. Therefore, it is very important to distinguish sedimentary and diagenetic structures from tectonic structures.

Typical diagenetic "enterolithic" folds and buckles are found at several positions of the Schafisheim core (e.g. Fig. 4a and DRONKERT et al. 1989). In most cases, sedimentary and diagenetic folds are open folds with upright fold planes showing irregular thickening and thinning of fold hinges and limbs. Anticlines of sedimentary and early diagenetic folds are often truncated. Slumping, which is quite common in evaporitic environments (Widmer 1989) produces reclined folds that may be confused with tectonic flow folds.

The scale is one important criterion to discern tectonic from sedimentary folding. All fold-like structures described by DRONKERT et al. (1989) that originated from the tectonically undisturbed foreland do not exceed a few decimeters. Therefore, we suggest that all structures larger than one meter have to be of tectonic origin e.g. the folded member II in the lower thrust sheet and the double fold within the salt layer (Figs. 3 and 4). At Schafisheim folding by dissolution may be excluded because of the absence of breccias, which are common in areas of dissolution (DRONKERT et al. 1989; Widmer 1989).

For all other folds and faults, a distinction may be difficult, because many tectonic structures probably had sedimentary precursors. Even when the geometry of such folds is tectonic, their tectonic origin may be doubtful because they are in the immediate vicinity of undeformed sedimentary structures (e.g. Fig. 7: slightly overprinted sedimentary structures on top of tectonic ones). Analysis of fold vergence with respect to overall deformation pattern, a good criterion for the recognition of tectonic structures in larger outcrops, fails because of the lack of reliable information on core orientation and surrounding deformation structures. Good criteria for the recognition of tectonic structures are the rheological behavior of the different lithologies and the microstructure of the anhydrite. Micrographs from the fold in Fig. 5 show elongation of anhydrite grains parallel to axial plains (Figs. 6a and b). Although the fabric was post-kinematically recrystallized, the preferred orientation is still preserved. No hydration or dehydration took place after folding, which may have destroyed the fabric. Therefore, this fold developed or was at least enhanced under conditions where anhydrite is the stable form of calcium sulphate, i.e. outside the sedimentary domain. Another criterion that excludes sedimentary folding is the differing rheological behavior between pure and impure anhydrite (Fig. 5 ff.). Based on experimental work on wet shales (NÜESCH 1989), we suggest that there is no significant difference in rheology between sulphate and carbonate muds. On the other hand, in some of the structures presented here (e.g. Figs. 5 and 6), the impure (carbonatic, quartz- and clay-bearing) anhydrite behaves brittly in contrast to highly ductile pure anhydrite (cf. Fig. 6c).

Boudinage of carbonate-bearing layers in anhydrites

Boudinage of carbonate-bearing layers is common not only throughout the whole Schafisheim sequence but also in other tectonized evaporites (e.g. BORNS 1983, JOR-

DAN 1988b). In Fig. 9 the relatively thin magnesitic layer 1 (Table 1), sandwiched between nearly pure anhydrites, is boudinaged parallel to layering. The boudin necks are filled with halite (H in Fig. 9), and very pure anhydrite respectively (Fig. 10). The original anhydrite fibre-texture, which runs parallel to layering, is often altered by post-kinematic static recrystallization. However, the existence of these pure anhydrite extension veins confirms that the boudins are caused by tectonic stretching and not by synsedimentary or diagenetic processes like e.g. dessication. Some of the boudins were imbricated (Figs. 9, 10b and 11). Overthrusting of carbonatic layers postdates the boudinage as shown by the sheared extension vein in Fig. 10b. We conclude that boudinage and its inversion are associated with successive stages of layer parallel shearing during detachment and folding.

Flow and mylonization of anhydrites

In all samples, strong elongated anhydrite fabrics (Fig. 6b) or pronounced textures (Fig. 8b) document high strains. However, equilibrated grain boundaries imply post-kinematic alteration of the microstructure by static recrystallization (e.g. Figs. 6 and 10), and, therefore, the mechanisms responsible for flow of anhydrite may not be determined. Nevertheless, many Schafisheim samples show great analogies in deformation structures, fabric, texture, and grain size distribution to post-kinematically unrecrystallized anhydrites from the Jura proper (Belchen motorway tunnel) where twinning, intra-crystalline glide, and syn-kinematic recrystallization by grain boundary migration are recognized (JORDAN 1988b). These findings agree with experimental evidence of MÜLLER et al. (1981).

In the lower part of core sample 2 (Fig. 7), recumbent isoclinal flow-folds document a high shear deformation, which reaches a maximum at the bottom of the core sample. Nevertheless, the corresponding micrographs (Fig. 8b) show a weakly elongated grain fabric in comparison. Anhydrite from significantly less sheared samples provide much more pronounced grain fabrics (e.g. Fig. 6). Again, the equilibrated grain boundaries document weak postkinematic recrystallization. But in analogy to the preserved axial-plane-parallel fabric of various folds (e.g. Fig. 6), we feel that the present grain fabric is not fully annealed. This view is supported by the slight elongation and the distinct preferred orientation of the grains. Also, the fabric of this very pure anhydrite does not resemble original sedimentary or diagenetic fabrics (H. Dronkert, pers. comm. 1988) but bears a striking resemblance to mylonitic fabrics known from calcite mylonites etc. (e.g. SCHMID 1982; cf. MÜLLER et al. 1981). Further investigations are in progress.

Both, folded (Fig. 6c) and boudinaged sequences (Figs. 9 to 11) imply that carbonatic layers were increasingly more competent with increasing carbonate content. Layers with only 25% impurities were often brittle adjacent to ductile pure anhydrites (layer 1 in Fig. 5). Within graded, carbonate-bearing horizons, anhydrite occurs mostly in the form of "anhydrite laths" (lamellae in three dimensions). In folds, these laths are bent around the fold axes, while within the adjacent pure anhydrite the grains are elongated parallel to the axial plane (e.g. Fig. 6d). The laths show the original pre-kinematical fabric, while the fabric within the pure anhydrite is completely rearranged by intracrystalline deformation and syn-kinematic grain boundary migration. We suggest that

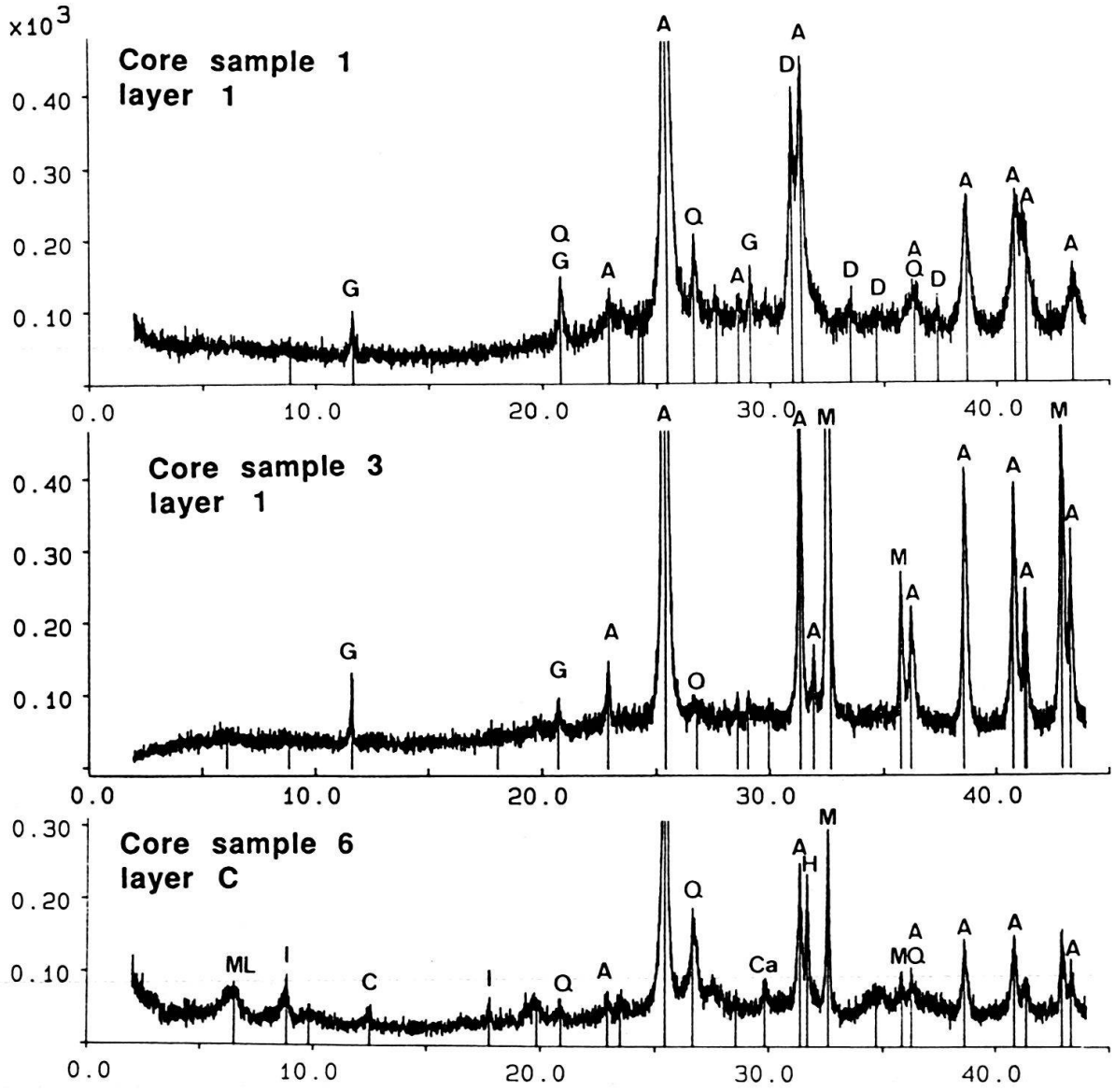

Fig. 14. X-ray diffractograms of the air-dried sulphate suspension from core samples 1, 3 and 6 (cf. Table 1). The following abbreviations have been used: ML (mixed layers), I (illite), CL (chlorite), A (anhydrite), G (gypsum), M (magnesite), D (dolomite), C (calcite), H (halite) and Q (quartz).

within the carbonatic horizons, a corresponding anhydrite deformation was hindered or limited by the presence of fine-grained dolomite or magnesite grains. The presence of dolomite results in an additional increase in strength by rigid inclusions in addition to the increase caused by geometrodynamical effects only (Jordan 1988a).

A special remark on the mineralogy of the evaporites

Besides variations in mineralogy between the various layers, we have found a noteworthy systematic variation between core sample 1 and 2 of the (upper) "layered sulpharenites (IIIb) and core sample 3 and 6 from the double fold of the "salt layers"

which possibly is a relict or equivalent of the (lower) "layered sulpharenites" (IVb). In member IIIb, dolomite was the only carbonate, while in the lower sequence (? IVb), magnesite is common, calcite is rare and dolomite is absent (Fig. 14 and Table 1) The grain size of both dolomite and magnesite is very small compared to anhydrite. The influence of the two carbonates on the rheology of anhydrite is comparable. Until now, magnesite was not described from the Muschelkalk evaporites of Switzerland. In some previous works, it was confused with dolomite (K. Ramsayer, pers. comm. 1988). Possibly, magnesite may be used as a marker mineral for the member IVb.

Conclusions

1) Anhydrite flowed under the ambient conditions effective at Schafisheim during Jura overthrusting. However, the deformation mechanisms that were effective during flow cannot be determined for certain because of post-kinematic equilibration of the grain fabric. Nevertheless, if we consider strain rate ($1.3 \cdot 10^{-12}$ s^{-1} and $1.8 \cdot 10^{-13}$ s^{-1}) and paleotemperature (70–78 °C) at the time of overthrusting, then the flow strength of naturally deformed anhydrite may be even lower than the values resulting from the extrapolation of experimental data (Müller et al. 1981).

2) The strength of anhydrite increases with very small amounts of impurities. In the case of Schafisheim, these impurities are very fine-grained dolomites or magnesites.

3) A considerable amount of shear is concentrated within highly deformed anhydrites with a mylonite-like fabric. At Schafisheim, such anhydrite tectonites occur predominantly within the layered sulpharenites (member IIIb). This is quite surprising because these tectonites formed directly above thick layers of weaker rocksalt. The existence of anhydrite tectonites suggest that Jura detachment took place, at least partly, within the anhydrites as suggested by Laubscher (1961) and Müller & Hsü (1981).

Acknowledgments

Our work has benefited from hints and constructive criticism by Hans Dronkert, Walter Müller, Dave Olgaard, Karl Ramseyer, Stefan Schmid, and Thomas Widmer. W.H. Müller of Nagra, Baden, kindly provided the core sections. For help in mineralogical investigations we like to thank Max Müller-Vonmoos, Fritz Madsen, and Günter Kahr. The present work was partly supported by Swiss National Foundation, project No. 2.324–0.86. Special thanks to Christoph Lüthy.

REFERENCES

Baumann, W. 1984: Rheologische Untersuchungen an Gips. Eclogae geol. Helv. 77/2, 301–325.

Borns D.J. 1983: Petrographic study of evaporite deformation near the waste isolation pilot plant (WIPP). Sandia Report, SAND 83–166, Sandia National Laboratories, Albuquerque and Livermore (USA).

Buxtorf, A. 1907: Zur Tektonik des Kettenjura. Ber. Versamml. oberrh. geol. ver. 30/40. Versamml. 1906/1907, 29–38.

Diebold, P. & Müller, W.H. 1985: Szenarien geologischer Langzeitsicherheit: Risikoanalyse für ein Endlager für hochradioaktive Abfälle in der Nordschweiz. NTB 84–26, Nagra, Baden (Switzerland).

Dronkert, H. 1987: Diagenesis of Triassic evaporites in northern Switzerland. Eclogae geol. Helv. 80/2, 397–414.

Dronkert, H., Matter, A. & Bläsi, H.-R. 1989: Facies and origin of Triassic evaporites from Nagra boreholes, Northern Switzerland. Beitr. geol. Karte Schweiz (in press).

Jordan, P. 1987a: The deformational behavior of bimineralic limestone-halite aggregates. Tectonophysics 135, 185–197.
— 1987b: Eine Methode zur Abschätzung tektonischer Scherraten aufgrund mikrostruktureller Beobachtungen. Eclogae geol. Helv. 80/2, 491–508.
— 1988a: The rheology of polymineralic rocks – an approach. Geol. Rdsch. 77/1, 285–294.
— 1988b: Deformationsstrukturen in den Keuper-Evaporiten des Belchen-Tunnels (Faltenjura, Schweiz). In: Gosen, W. von (Ed.): Sonderband TSK II Erlangen 1988, Erlanger Geol. Abh. 116, 53–66.
Laubscher, H.P. 1961: Die Fernschubhypothese der Jurafaltung. Eclogae geol. Helv. 54/2, 221–282.
— 1975: Viscous components in Jura folding. Tectonophysics 27, 239–254.
— 1980: Die Entwicklung des Faltenjuras. Daten und Vorstellungen. N. Jb. Geol. Paläont. Abh. 160, 289–320.
— 1984: Sulfate deformation in the upper Triassic of the Belchen tunnel (Jura Mountains, Switzerland). Eclogae geol. Helv. 77/2, 249–259.
Matter, A., Peters, Tj., Bläsi, H.-R., Schenker, F. & Weiss, H.-P. (1988): Sondierbohrung Schafisheim – Geologie. NTB 86–03, Nagra, Baden (Switzerland).
Müller, W.H., Blümling, P., Becker, A. & Clauss, B. 1987: Die Entkoppelung des tektonischen Spannungsfeldes an der Juraüberschiebung. Eclogae geol. Helv. 80/2, 473–489.
Müller, W.H. & Hsü, K.J. 1980: Stress distribution in overthrusting slabs and mechanics of Jura deformation. Rock Mech., Suppl. 9, 219–232.
Müller, W.H., Huber, M., Isler, A. & Kleboth, P. 1984: Erläuterungen zur «Geologischen Karte der zentralen Nordschweiz 1:100 000». NTB 84–25, Nagra, Baden.
Müller, W.H., Schmid, S.M. & Briegel, U. 1981: Deformation experiments on anhydrite rocks of differente grainsize: rheology and microfabric. Tectonophisics 78, 527–543.
Naef, Hch., Diebold, P. & Schlanke, S. 1985: Sedimentation und Tektonik im Tertiär der Nordschweiz. NTB 85–14, Nagra, Baden (Switzerland).
Nüesch, R. 1989: Das mechanische Verhalten von Opalinuston. Ph. D. thesis ETH Zürich.
Ramseyer, K. 1987: Diagenese des Buntsandsteins und ihre Beziehung zur tektonischen Entwicklung der Nordschweiz. Eclogae geol. Helv. 80/2, 383–398.
Schmid, S.M. 1982: Laboratory experiments on the rheology and the deformation mechanisms in calcite rocks and their application to studies in the field. Mitt. geol. Inst. ETH u. Univ. Zürich N.F. 241.
Sprecher, C. & Müller, W.H. 1986: Geophysikalisches Untersuchungsprogramm Nordschweiz: Reflexionsseismik 82. NTB 84–15. Nagra, Baden.
Weber, H.P., Sattel, G. & Sprecher, C. 1986: Sondierbohrungen Weiach, Riniken, Schafisheim, Kaisten, Leuggern: Geophysikalische Daten. NTB 85–50. Nagra, Baden.
Widmer, T. 1989: Zur Stratigraphie und Sedimentologie der Anhydritgruppe (Mittlere Trias) in der Region Liestal–Arisdorf (Baselland, Nordwestschweiz). Unpubl. Ph. D. thesis, Univ. Basel.
Wohnlich, H.M. 1967: Kleintektonische Bruch- und Fliessdeformation im Faltenjura. Unpubl. Ph. D. thesis Univ. Basel.

Manuscript received 18 May 1988
Revision accepted 20 December 1988